Microelectronics Reliability 58 (2016) 95–102

Contents lists available at ScienceDirect

Microelectronics Reliability

journal homepage: www.elsevier.com/locate/mr

Reliability of photovoltaic systems using seasonal mission profiles and the FIDES methodology☆

Susana de Leon, Hugo Calleja *, Jesus Mina

National center for research and development of technology, Electronics department, Interior Internado Palmira s/n, Cuernavaca, Morelos, C.P. 62490, Mexico

ARTICLE INFO

Article history:
Received 26 June 2015
Received in revised form 23 November 2015
Accepted 30 November 2015
Available online 7 December 2015

Keywords:
Reliability prediction
Mission profile
Photovoltaic systems

ABSTRACT

In areas with hot weather, photovoltaic systems can be used to help relieve the peak demand caused by air conditioning equipment. Users, however, are reluctant to invest in solar technology, arguing that the equipment commercially available is unreliable because it was developed for others environments. In this paper, the reliability assessment of a DC/DC converter aimed at PV applications is presented. The reliability estimation was performed following the FIDES methodology, taking into account seasonal mission profiles developed for five specific sites for which there is meteorological data available. The goal was to identify the most failure prone components, and the dominant stress factors. It was found that the smallest contribution to the failure rate occurs during winter. The largest contribution occurs in spring or summer, depending on the site. In the converter, the most failure-prone components were the diodes, which contributed with about 70% of the overall failure rate.

1. Introduction

Currently, there are efforts under way aimed at fostering the widespread installation of photovoltaic (PV) systems in Mexico. The goal is to help relieve the power demand caused by air conditioning equipment. Many potential users, however, are reluctant to invest in solar technology because there is a perception that PV systems are unreliable, a common remark being that they were developed with other environments in mind.

One of the major requirements of probabilistic design for reliability is that "Design efforts should be specific for a product, and their most likely actual or anticipated applications" [1,2]. In the case of photovoltaic systems, this might be a difficult requirement to comply with because, at a daily basis, the power circuit operating point evolves from minimum load up to a maximum, and then back to minimum. Further, they are often installed outdoors, subject to daily and seasonal weather variations. As a result, efficiency, reliability, and other performance parameters of PV systems depend on the installation site [3–5].

The power electronics converter is usually the most failure-prone assembly [6–8]. It has been found that the dominant deterioration mechanism in semiconductor devices is usually linked to effects such as long-term exposure to high temperatures and thermal cycling, which produces thermo-mechanical stresses due to the difference in expansion coefficients [9–12]. These mechanisms depends both on environmental and operation conditions [13].

Design efforts should be oriented in such a way that the converter operational life is lengthened. These efforts usually require an assessment of the reliability taking into account, as much as possible, realistic information about the installation site. There are several options available for the assessment [14]. The procedure described in the Military Handbook 217F [15] has been widely used to predict the reliability of components in power electronics converters [16–18]. A drawback of this approach (and other that share the same philosophy), however, is that they rely on statistical data collected throughout the years. Therefore, reliability predictions are biased by data that applies to old components, often yielding over-pessimistic estimation [19]. A better approach that explicitly takes into account the mission profile is the FIDES methodology [20–23]. It has been found that this method yields results that match field data with an acceptable deviation [24].

It has already been shown that thermal stresses, and therefore contributions to the overall failure rate, are rather small at low irradiance levels [25]. The results reported, however, assumed a yearly mission profile, and did not take into account seasonal changes of irradiance, temperature and humidity. In this paper, the analysis is taken one step further, to include seasonal variations. The assessment of the reliability of a DC/DC converter aimed at a photovoltaic system, using seasonal mission profiles is described herein. Reliability is estimated following the FIDES methodology. Several sites were selected for the assessment. The results were compared to identify seasonal trends. The southernmost latitude considered is N 15.67°, and the northernmost is N 32.63°. The most failure-prone components within the converter were also identified. The ultimate goal is to provide manufacturers with reliability information that can be helpful in developing more robust systems.

☆ Special Issue on *Reliability issues in Power Electronics*, 2015.
* Corresponding author.

http://dx.doi.org/10.1016/j.microrel.2015.11.023
0026-2714/

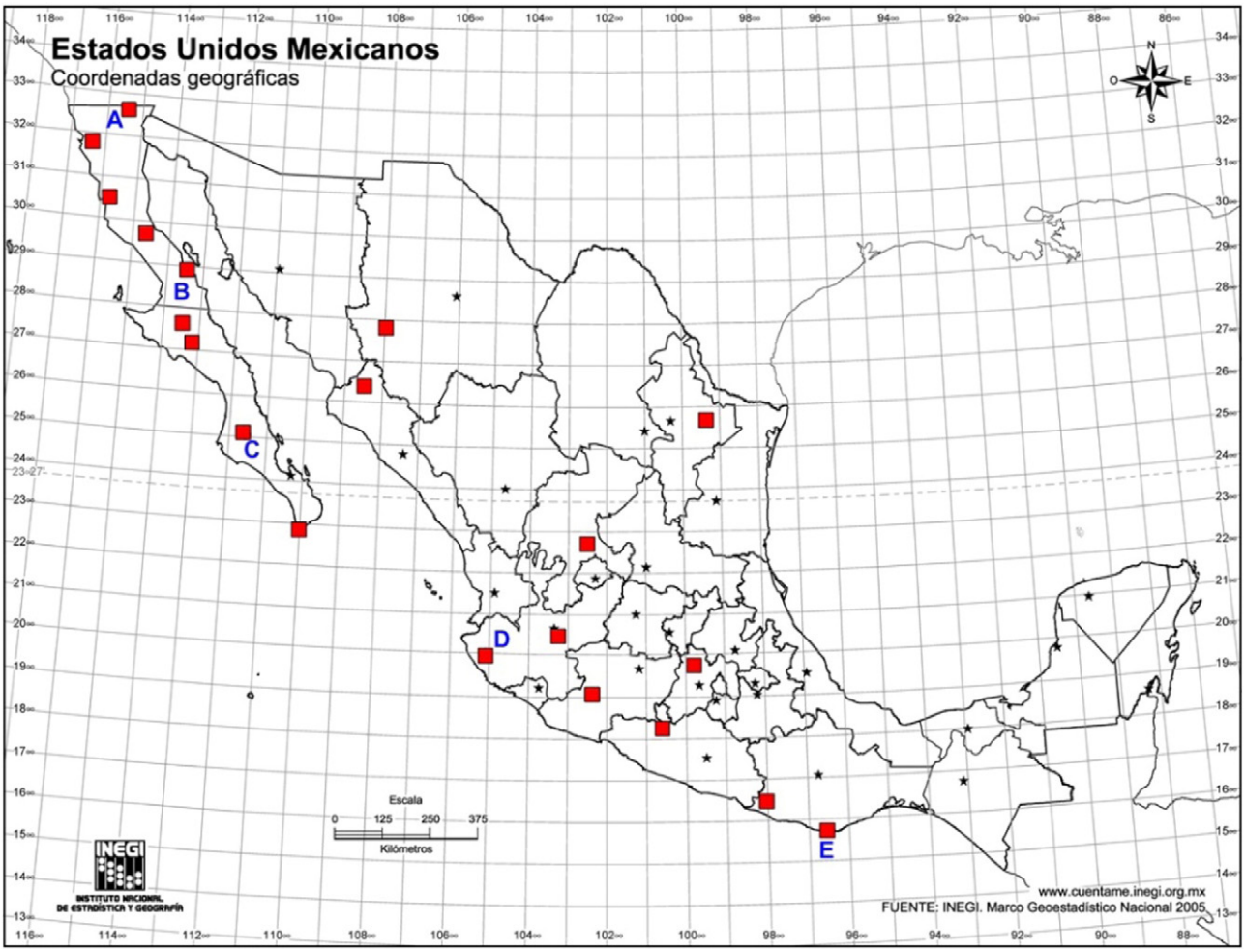

Fig. 1. Test sites.

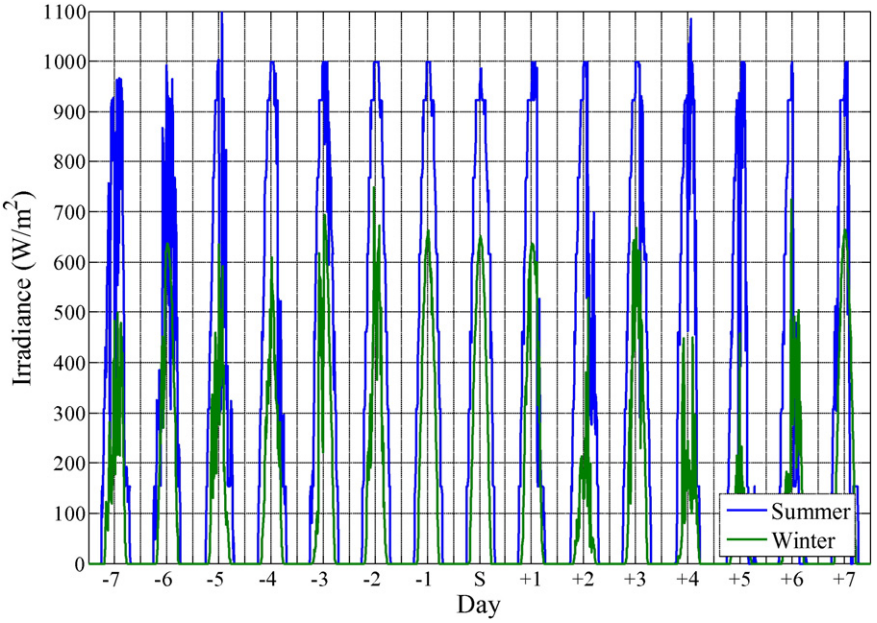

Fig. 2. Site E: daily irradiance around summer and winter solstices.

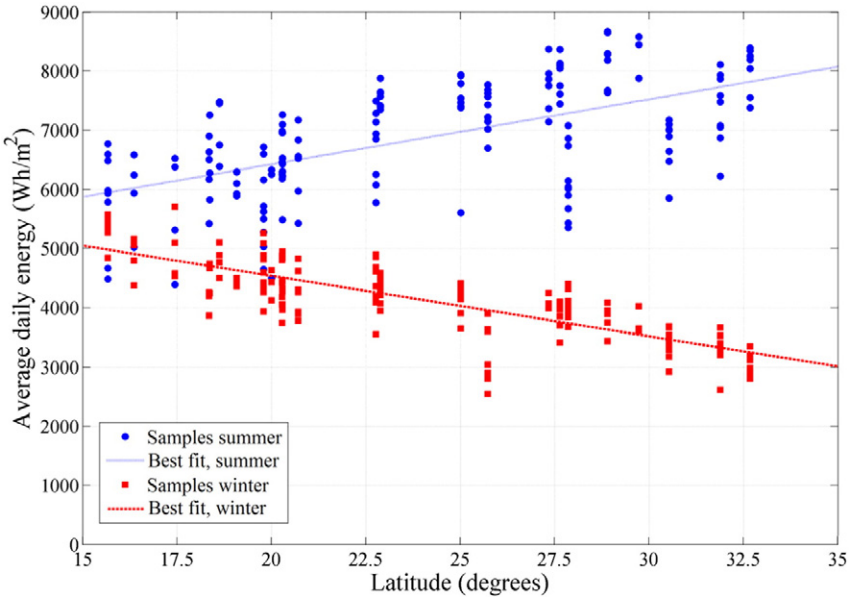

Fig. 3. Average daily energy in summer, and in winter.

2. The FIDES methodology

Reliability information is usually conveyed in terms of the failure rate λ. In the FIDES methodology the failure rate of any item is expressed as [20]:

$$\lambda = \pi_{pm}\pi_{process}\lambda_{phy} \tag{1}$$

where π_{pm} is the stress factor associated to the quality and technical control over manufacturing of the item. The term $\pi_{process}$ involves all processes that can be linked to the item, from specification to maintenance. The last term, λ_{phy}, takes into account all the phases that occur during the operation of the item. It is given by:

$$\lambda_{phy} = \sum_i^{Phases} \left[\frac{t_{annual}}{8760}\right]_i \pi_i\lambda_i \tag{2}$$

where t_{annual} is the annual duration of the i'th phase. The term π_i is the induced overstress factor (electrical, mechanical or thermal), and is given by:

$$\pi_i = \left(\pi_{placement}\pi_{app}\pi_{rugg}\right)^{0.511 \quad \ln\left(C_{sensitivity}\right)} \tag{3}$$

The terms within the brackets, defined by the user, are specific to the component and the application. The failure rate λ_i, which applies to the i'th phase, is subdivided into k contributions, each one including usually a component-specific base failure rate λ_{0k}, multiplied by an acceleration factor π_k that indicates the sensitivity to operational and environmental conditions:

$$\lambda_i = \Sigma_k\lambda_{0k}\pi_k \tag{4}$$

The acceleration factors indicate the magnitudes of physical constraints on the component during operational or dormant phases. The

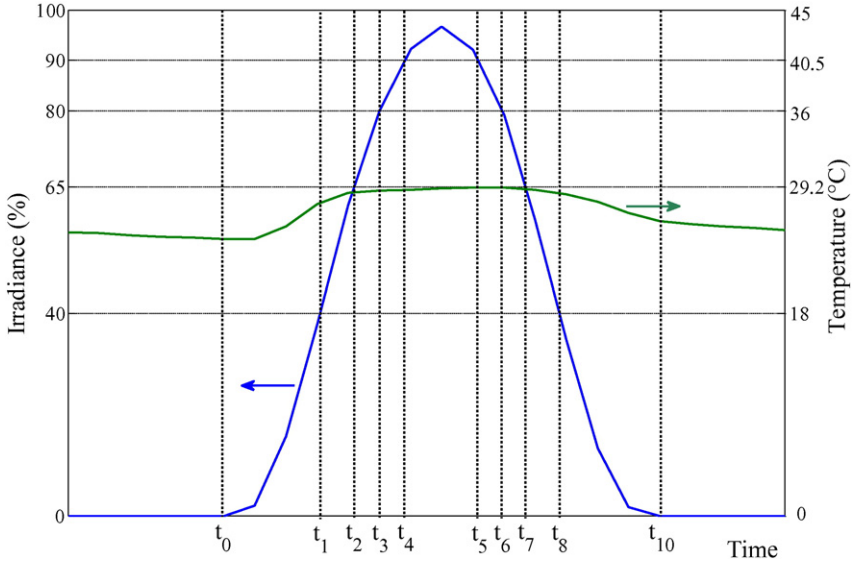

Fig. 4. Operational phases in the mission profile.

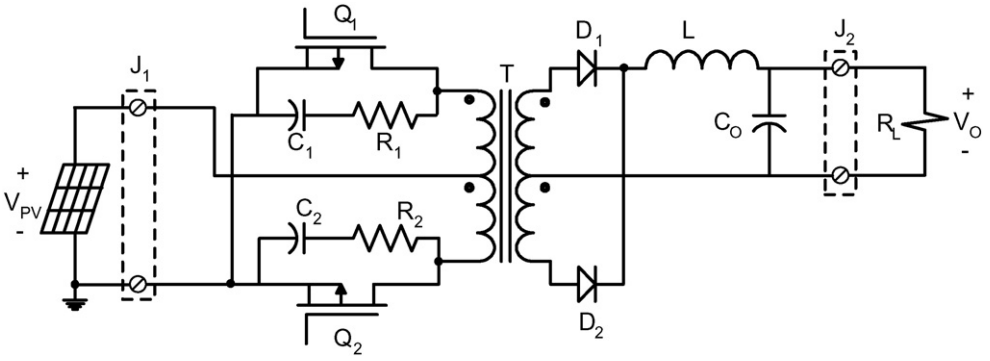

Fig. 5. Power converter.

constraints on λ_i can be thermal, case and solder joints related (both factors depending on the temperature gradient applied to the component during the given phase), humidity related, and mechanical stresses.

3. Mission profile

The so-called mission profile can be defined as "time-phased description of the events and environments an item experiences from initiation to completion of a specified mission" [26]. The information required to specify a mission profile includes the number of phases, its individual lengths t_{annual}, and the stresses (thermal, mechanical, and humidity related) on the items during each phase. This information can be obtained from meteorological data collected in the installation site.

In the case presented herein, it is assumed that the PV converter is installed in a "ground-fixed" environment, and that pollution is nonexistent. Therefore, the data taken into account should include irradiance, temperature, and relative humidity.

3.1. Seasonal variations

A characteristic of inverters in PV systems is that the operating point evolves from a minimum, early in the morning, up to a maximum, and then back to minimum, at dusk. At any specific date, both the maximum irradiance and the length of the cycle depend on the installation site. Further, the stresses on the inverter, and thus its reliability, depend on the amount of energy processed in it.

An average yearly value could be used to assess the reliability of the inverter, but there might be significant differences between locations and seasons. The sites marked in the map in Fig. 1. were chosen to clarify this issue. They are spread throughout a span of 17 degrees of latitude, and were selected because there is a data base of meteorological measurements available, covering at least 5 years for some locations, and up to 10 years for others. Meteorological variables were measured at facilities of the national utility company, and the results provided to participants in the research project mentioned in the acknowledgements section. The measurements provided included ten-minutes averages of temperature, irradiance and relative humidity.

The maximum yearly difference in the daily energy handled by the inverter depends upon the differences in irradiance, and lengths of the diurnal cycles between summer and winter. This is exemplified by Fig. 2, obtained for the site labeled as "E", and corresponding to 15-days periods: one centered in the summer solstice (blue line) and the other in the winter solstice (green line). The difference between summer and winter can be readily appreciated. For the days shown, the average summer irradiance is 571 W/m^2, while the average winter irradiance is 280 W/m^2.

Fig. 3 shows the average daily energy in the sites shown on the map. Each point was obtained averaging the 15-days period centered in the corresponding solstice, per installation site and per year. The dotted lines shown correspond to the best-fit linear approximations for summer and winter samples, as a function of latitude.

As can be seen, for the southernmost location the difference between summer and winter is rather small, approximately 20% in the linear approximation shown by the dotted lines. In contrast, the difference is quite large in the northernmost location, with a ratio of about 1:2.5 between winter and summer. Since thermal stresses on the converter depend on the amount of energy processed, it seems advisable to use a seasonal mission profile for northern locations. Location in the south might not need such degree of detail, but at this point it is not clear if this is indeed the case. Therefore, seasonal mission profiles will be used.

3.2. Operational phases

Within the geographical region considered, thermal stresses are rather small at low irradiance levels [25]. Therefore, a mission profile with 5 levels is selected, each level corresponding to an operational phase.

The maximum level for each test site is obtained as the irradiance value that corresponds to a 99.5% of the cumulative frequency function. As shown in Fig. 4, the first level spans from 0% to 40%. The second spans from 40% to 65%. The third from 65% to 80%, the forth from 80% to 90%, and the fifth from 90% to 100%. There will be an additional phase corresponding to the dormant condition. Therefore, for each season, the mission profile will include six phases.

Referring to Fig. 4, the temperature values required by the FIDES methodology are calculated, on a daily basis, for each of the lapses shown (t_0 - t_1, t_1 - t_2, t_2 - t_3, and so forth). Afterwards, the daily results are averaged to yield seasonal values. The curve corresponding to humidity is not shown, but the values required by the FIDES procedure are obtained in a similar manner. Data for each phase include its duration, average temperature, maximum change in temperature, and average relative humidity.

4. DC/DC Converter

The DC/DC converter used for evaluation purposes is shown in Fig. 5. This configuration was selected mainly because, for safety reasons, regulations require galvanic isolation to avoid leakage ground currents through the solar panel parasitic capacitance. The converter is suitable

Table 1
Locations of test sites.

Label	Site	Latitude N	Longitude W
A	Mexicali	32.67	115.29
B	Bahía de los Ángeles	28.90	113.56
C	Cd. Constitución	25.01	111.66
D	Tomatlán	20.00	105.13
E	Puerto Ángel	15.67	96.50

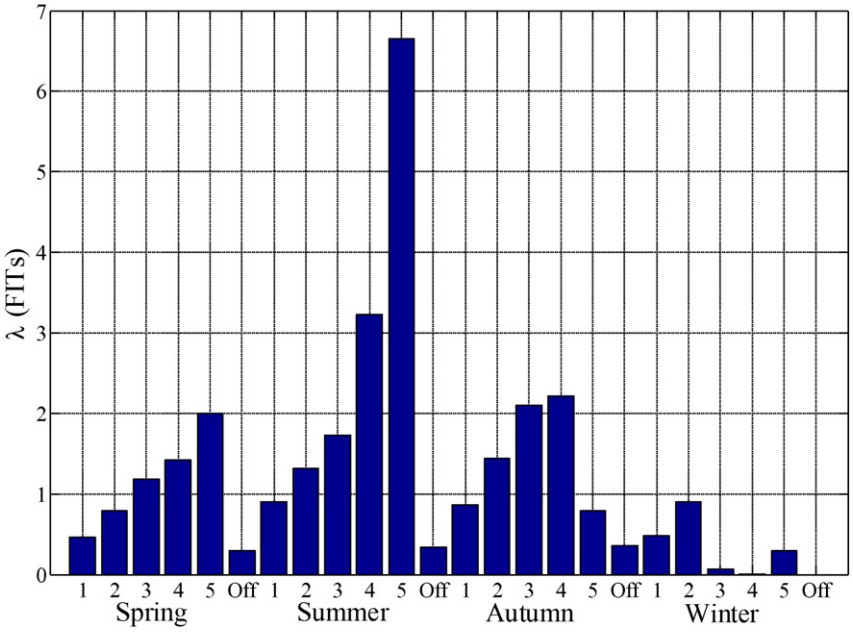

Fig. 6. Failure rates at the northernmost location (Mexicali).

for applications not requiring an AC voltage, with high current and low DC voltage at the input side (e.g. battery sourcing applications, standalone PV systems, and telemetry applications, etc.). The converter was built with diodes rated at $V_R = 600$ V, and $I_{F(AV)} = 15$ A. The transistors were rated at $V_{DSS} = 55$ V and $R_{DS(on)} = 8$ mΩ. In isolated converters such as the push-pull configuration, the main switches suffer from high voltage spikes and power losses due to the leakage inductance of the transformer. A RC snubber network was added to overcome these issues. The DC/DC converter is rated at 100 W, a rating in the range of modular integrated converters. The panel is rated at $V_{PV} = 17.5$ V, and $V_O = 48$ V.

If the characteristics of the PV panel at the input are known, then the power at the converter can be related to the environmental data using:

$$P_{PV} = \frac{E_e}{E_o} P_{MO}[1 + \gamma(T - T_O)] \tag{5}$$

where E_O and T_O are irradiance and temperature at STC. P_{MO} is the corresponding power, also at STC, and γ is the temperature coefficient. In turn, P_{PV}, T and E_e are the actual output power, temperature and irradiance. The converter was fully characterized, and the temperature and electrical stresses at different power levels have been recorded.

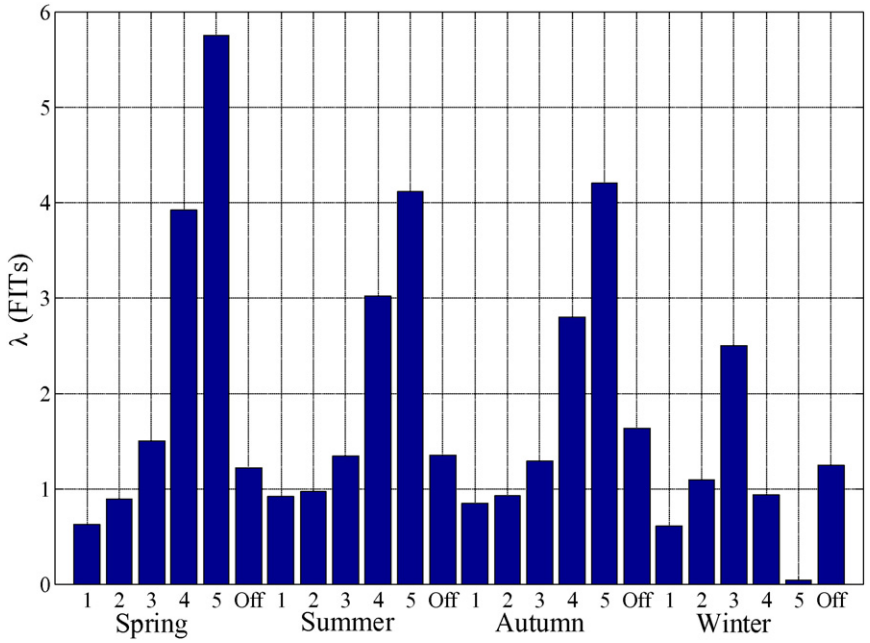

Fig. 7. Failure rates at the southernmost location (Puerto Ángel).

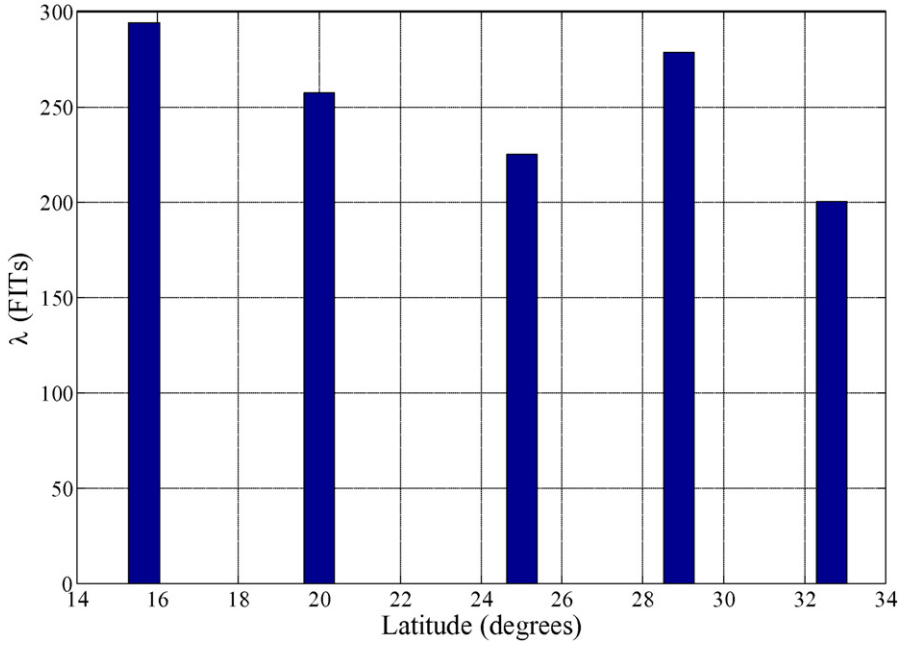

Fig. 8. Overall failure rates as a function of latitude.

5. Results

The performance of the DC/DC converter was assessed when connected to a polycrystalline panel rated at 125 W, with $\gamma = -0.485\%/°C$. Reliability results were obtained for locations labeled A through E in Fig. 1, at the geographic coordinates listed in Table 1. Meteorological data was available in W*indographer* format. The data was exported to a mathematical software package for number crunching, and a routine incorporating the panel characteristics was written to generate the mission profile. Afterwards, mission profile and converter data were fed to a software package that implements the FIDES methodology [27].

Results for location A are shown in Fig. 6. There is a set of six bars for each season, the one at the left corresponding to the phase with the lowest power level (labeled as "1"), and the one at the right to the dormant phase (labeled as "Off"). It can be seen the largest failure rate occurs in summer, at the phase corresponding to the highest power level. In contrast, winter contributions are rather small, and contribution from phases 4 and 5 are virtually null.

Fig. 7 depicts the results obtained for location E. Within a season, the contributions of the individual phases exhibit the same trend found in Fig. 6. In a yearly basis, the lowest contribution also occurs in winter, but the highest contribution occurs in spring. Fig. 8 shows the overall failure rates for the five test sites, as a function of latitude.

Fig. 9 shows the contributions of the individual components in the converter to the overall failure rate, expressed in FITs, including connectors J1 and J2, and the PCB. The plot corresponds to a single test site, but the percent proportions are very much the same for the other sites. The diodes at the output are, by far, the most failure-prone component, each one contributing with about 35% of the total failure rate. In contrast, the output capacitor C_o contributes with 9.5%. The transistors contribute with an average of 6.6% each.

The stress factor with the highest effect on the failure rates of the diodes is the thermal one, followed by a small contribution, less than 1%, from the relative humidity factor. In the output capacitor, the entire failure rate is linked to the thermo-electrical factor. In the transistors, the thermal factor accounts for 91% of the failure rate, followed by the relative humidity factor, with an average contribution of 8.5%.

According to manufacturers, failures in connectors can be related to a variety of causes [28]. Its operational lifetime is often limited by the effects of fretting [29]. However, since it is assumed that the converter is to be installed in ground, stationary environments, it is likely that most of the connector-related failures will be related to oxidation mechanisms, and to corrosion resulting from chemical stresses (which affects other components in the converter, including the PCB).

FIDES takes into account several contributing factors. Among them are the so-called application and environmental pollutions, both having weak, moderate or strong levels, (the former corresponding to operation in inhabitated, uninhabitated or engine zones; the latter corresponding to installation in rural, urban or industrial areas). The effects of these levels on reliability are numerically shown in Table 2, which lists the overall failure rate as a function of the environmental pollution stress factor π_{envir}, and the application pollution stress factor π_{zone}. The locations considered were those at latitude extremes. Changing from a

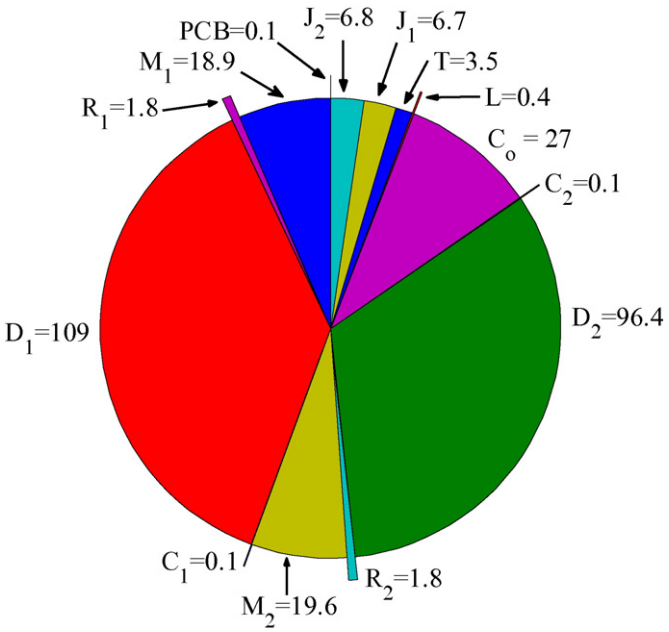

Fig. 9. Failure rates distribution.

Table 2
Failure rate (FITs) as a function of π_{envir}, and π_{zone}.

		π_{envir}		
	π_{zone}	Low	Moderate	High
Mexicali	Low	195.18	196.41	197.65
	Moderate	197.64	200.11	202.57
	High	202.58	207.51	212.44
Puerto Angel	Low	288.93	290.17	291.40
	Moderate	291.40	293.88	296.33
	High	296.33	301.27	306.20

low-low location to a *high-high* one can deteriorate the failure rate in as much as 9%.

Reliabity is also affected by salinity, expressed by the saline pollution level π_{sal}, which can be strong for coastal regions, and weak otherwise. The characteristics of the enclosure are taken into account by the product protection level stress factor π_{prot}, which can be either hermetic or non-hermetic. Table 3 lists the failures rates obtained with the different combinations of π_{sal} and π_{prot}. The calculation were again performed for the sites at the latitude extremes.

6. Comments and remarks

According to Fig. 3, the difference in average daily energy between summer and winter is small in southern locations. However, the failure rates in Fig. 7 show a much larger difference. Therefore, it seems advisable to use a seasonal mission profile instead of a yearly one. The difficulty to generate a seasonal mission profile for a specific site is in having a reliable data base available, encompassing at least one year. If the data is available, the synthesis of the mission profile is a relatively simple task.

From a seasonal point of view, winter produces to smallest contribution to the failure rate. The largest contribution occurs in summer (in dry, desert-like environments) or in spring. The contributions of the two remaining seasons (autumn and spring, or autumn and summer) are similar.

The results in Fig. 8 suggest a correlation between failure rates and latitude in test sites A, C, D, and E. Temperature and irradiance data was further analyzed in an attempt to find a simple correlation between these variables and the failure rate, but none was found. Clearly, this is due to the complexity of the equations involved in the reliability calculations.

Capacitors are often blamed as the most failure-prone components. In the converter analyzed, the average contribution of the capacitor to the overall failure rate is 11.2%. In contrast, the contribution of each diode is 35%. In diodes and transistors, the dominant stress factor is thermal. In the output capacitor (an electrolytic one), the dominant is the thermoelectrical factor. In the other passive components, the thermal cycling factor has a noticeable influence, from about 5% for the transformer, up to 25% for the snubber capacitors.

The effect of changing the diode package was also explored, switching from a TO-220 package (as was used in the results reported), to a D2PAK. The latter one provides a better performance form a humidity point of view. However, in the sites analyzed the improvement was very small, less than 1%. Nevertheless, devices in the D2PAK package should provide a better performance in high humidity environments.

Table 3
Failure rate (FITs) as a function of π_{sal} and π_{prot}.

		π_{prot}	
	π_{sal}	Non-hermetic	Hermetic
Mexicali	Low	196.41	192.71
	High	200.11	192.71
Puerto Angel	Low	290.10	286.46
	High	293.86	286.46

Derating adds longevity to electronic assemblies, and three types of derating are often used in practice: voltage, current, and power. For power diodes and transistors, the methodology followed herein does not require neither the current values nor the actual voltages applied to the devices (it assumes that they are used at its rated voltage, with $\pi_{EI} = 1$).

Failure rates are predicted using as input data the thermal resistance of the package, and the power dissipated during each operational phase. This implies that a power derating approach is better suited for power converters. According to this approach, solid state devices for the converter tested were selected in such a way as to minimize losses: low on-resistance and fast switching times for transistors, low forward voltage drop and fast reverse recovery for diodes (keeping in mind that maximum current and voltage ratings are not to be exceeded). Once components have been selected, reliability can be improved by using efficient heat management techniques. For the case in hand, the contribution from the diodes to the overall failure rate can be reduced by using a heatsink with a lower thermal resistance, although this will likely impact negatively on volume and weight.

For other components, such as capacitor and resistors, it is possible to successfully apply voltage derating. Suitable guidelines for high reliability applications have already been provided elsewhere [30,31].

When designing the PCB, it should be kept in mind that reliability is directly proportional to conductor spacing, and is also affected by the technology employed, with through-hole technology providing the best results. This can be explained by the fact that mature processes (and also recognized manufacturers) provide the lowest failure rate.

7. Conclusions

In this paper, the reliability assessment of a DC/DC converter aimed at PV applications is presented. The reliability estimation was performed following the FIDES methodology, taking into account seasonal mission profiles developed for five sites spread from latitudes N 15.67 to N 32.67. It was found that the smallest contribution to the failure rate occurs during winter. The largest contribution occurs in spring or summer, depending on the site. In the converter, the most failure-prone components were the diodes, which contributed with about 70% of the overall failure rate. Chemical stress factors also have an impact and reliability, and hermetic enclosures should be used whenever possible.

Ackowledgements

This work is supported by the National Council for Science and Technology (Conacyt), under grant FORDECyT 190,603.

References

[1] E. Suhir, Could electronics reliability be predicted, quantified and assured? Microelectron. Reliab. 53 (2013) 925–936.
[2] E. Suhir, When adequate and predictable reliability is imperative, Microelectron. Reliab. 52 (2012) 2342–2346.
[3] D. Li, G. Cheung, J. Lam, Analysis of the operational performance and efficiency characteristic for photovoltaic system in Hong Kong, Energy Convers. Manag. 46 (2005) 1107–1118.
[4] S. Kumar, N.M. Vichare, E. Dolev, M. Pecht, A health indicator method for degradation detection of electronic products, Microelectron. Reliab. 52 (2012) 439–445.
[5] F. Spertino, G. Graditi, Power conditioning units in grid-connected photovoltaic systems: a comparison with different technologies and wide range of power ratings, Sol. Energy 108 (2014) 219–229.
[6] A. Ahadi, N. Ghadimi, D. Mirabbasi, Reliability assessment for components of large scale photovoltaic systems, J. Power Sources 264 (2014) 211–219.
[7] G. Zini, C. Mangeant, J. Merten, Reliability of large-scale grid-connected photovoltaic systems, Renew. Energy 36 (2011) 2334–2340.
[8] P. Zhang, W. Li, S. Li, Y. Wang, W. Xiao, Reliability assessment of photovoltaic power systems: review of current status and future perspectives, Appl. Energy 104 (2013) 822–833.

[9] M. Meinhardt, V. Leonavicius, J. Flannery, S.C. Ó mathúna. Impact of power electronics packaging on the reliability of grid connected photovoltaic converters for outdoor applications, Microelectron. Reliab. 39 (1999) 1461–1472.
[10] C. Busca, R. Teodorescu, F. Blaabjerg, S. Munk-Nielsen, L. Helle, T. Abeyasekera, P. Rodriguez, An overview of the reliability prediction related aspects of high power IGBTs in wind power applications, Microelectron. Reliab. 51 (2011) 1903–1907.
[11] M. Arifujjaman, Reliability comparison of power electronic converters for grid-connected 1.5 kW wind energy conversion system. Renewable Energy 57 (2013) 348–357.
[12] M. Musallam, C. Yin, C. Bailey, C. Mark Johnson, Application of coupled electro-thermal and physics-of-failure-based analysis to the design of accelerated life tests for power modules, Microelectron. Reliab. 54 (2014) 172–181.
[13] P. Tamilselvan, P. Wang, M. Pecht, A multi-attribute classification fusion system for insulated gate bipolar transistor diagnostics, Microelectron. Reliab. 53 (2013) 1117–1129.
[14] B. Foucher, J. Boullie, B. Meslet, D. Das, A review of reliability prediction methods for electronic devices, Microelectron. Reliab. 42 (2002) 1155–1162.
[15] Department of Defense, Military Handbook: Reliability prediction of electronic equipment, MIL-HDBK-217F, December 1991.
[16] G. Graditi, G. Adinolfi, G.M. Tina, Photovoltaic optimizer boost converters: temperature influence and electro-thermal design, Appl. Energy 115 (2014) 140–150.
[17] G. Graditi, D. Colonnese, N. Femia, Efficiency and reliability comparison of DC-DC converters for single phase grid connected photovoltaic inverters, SPEEDAM, 2010.
[18] F. Chan, F.H. Calleja, E. Martinez, Grid connected PV systems: a reliability based comparison, IEEE international symposium on Industrial electronics 2006, pp. 1583–1588.
[19] C. Jais, B. Werner, D. Das, Reliability Predictions – Continued Reliance on a Misleading Approach, IEEE symposium on Reliability and maintainability 2013, pp. 1–6.
[20] FIDES Guide 2009. Reliability methodology for electronics systems. FIDES Group; 2009.
[21] P. Charpenel, F. Davenel, R. Digout, M. Giraudeau, M. Glade, J.P. Guerveno, N. Guillet, A.A. Lauriac, S. Male, D. Manteigas, R. Meister, E. Moreau, D. Perie, F. Relmy-madinska, P. Retailleau, The right way to assess electronic system reliability: FIDES. Microelectronics Reliability. 43 (2003) 1401–1404.
[22] J. Marin, R. Pollard, Experience Report on the FIDES Reliability Prediction Method, IEEE symposium on Reliability and maintainability 2005, pp. 8–13.
[23] M. Bendali, C. Laroucl, T. Azlb, C. Marchand, G. Coquery, Reliability assesment in the design of interleaved converters under multi-physical constraints, IEEE International symposium on Industrial electronics 2014, pp. 2117–2121.
[24] M.K. Fritz, Comparison and evaluation of newest failure rate prediction models: FIDES and RIAC 217Plus, Microelectronics Reliability 49 (2009) 967–971.
[25] S. de León, H. Calleja, J. Aguayo, Reliability and mission profiles of photovoltaic systems: a FIDES approach, IEEE Transactions on Power Electronics 30 (2015) 2578–2586.
[26] Department of Defense, Military Standard Mil-Std-721C, Definition of terms for reliability and maintainability, 1970.
[27] Lambda Predict (version 9.0.9) [Computer Software]
[28] R.S. Mroczkowski, Connector Design/Materials and Connector Reliability, AMP Incorporated Technical Paper, 1993.
[29] M.I. Bâzu, T.M.I. Bâjenescu, Failure Analysis: A Practical Guide for Manufacturers of Electronic Components and Systems, John Wiley & Sons, 2011.
[30] Space product assurance: Derating - EEE components (ECSS-Q-ST-30-11C Rev 1), ECSSA European Cooperation for Space Standarization Secretariat, Requirements & Standards Division, 2011 Available at https://escies.org/webdocument/showArticle?id=167&groupid=6 (verified on October 2015).
[31] EEE-INST-002: Instructions for EEE Parts Selection, Screening, Qualification, and Derating (NASA/TP—2003–212242), Addendum, 2008, National Aeronautics and Space Administration, 2003 Available at http://nepp.nasa.gov/docuploads/FFB52B88-36AE-4378-A05B2C084B5EE2CC/EEE-INST-002_add1.pdf (verified on October, 2015).